CHAPTER VI
MODIFICATION OF ETHYLENE (VINYL ACETATE)-G-POLYLACTIDE

6.1 Abstract

From the previous work, in order to improve the compatibility between homo-PLA and homo-EVA phases, lactide monomer (LA) was introduced to the system as the initiator in graft copolymerization reaction of PLA onto the modified EVA chains. Moreover, the twin-screw extruder with 5 mixing zones was used in the production to increase mixing efficiency. The reaction was done via catalytic reactive extrusion with various $Sn(Oct)_2$ catalyst contents, various screw speeds and two different twin-screw extruders. Thermal properties, morphology, and physical properties of the modified EVA-g-PLA were studied.

keywords : Reactive extrusion, graft copolymerization, EVA-g-PLA

6.2 Introduction

Polylactide (PLA) is benefit from its biodegradability and biocompatibility, which suitable for packaging and/or medical uses. Moreover, PLA also has good mechanical, thermal and biodegradable properties. Those properties make PLA an attractive biopolymer for environmental concern [1]. However, flexural properties, heat distortion temperature (HDT), gas permeability, impact strength, melt viscosity for processing, etc. are not good enough in applications like packaging [2,3]. Therefore, copolymerization with other polymer is one of the PLA modificaton methods. In this work, graft copolymerization of polylactide onto ethylene (vinyl acetate) or EVA by using catalytic reactive extrusion was selected due to the biocompatibility and elastic properties of EVA, which can enhance the flexibility of PLA [4]. Moreover, the product also can be used as a compatibilizer in polymer blends [5].

There are two key reactions involving in preparation of graft copolymer by reactive extrusion. One is grafting reaction; grafting in an extruder reactor involves reaction of a molten polymer with a monomer or mixture of monomers capable of forming grafts to the polymer backbone. The second one is interchain copolymer

formation, which can be defined as reaction of two (or more) homopolymers to form copolymer. In the majority of cases the process involves combination of reactive groups of one polymer with reactive groups on a second polymer to form a block or graft copolymer. The process is usually run simply by intensive mixing of a melt of the two polymers in the extruder. Compatibilization of two immiscible polymers may be obtained through the presence of a block or graft copolymer of the two homopolymers, which present at the interface of the two immiscible phases and acts as an emulsifying agent and lowers interfacial tension. Block or graft copolymers are most economically formed by reactive extrusion to form covalent or, less commonly, ionic bonds [6].

This chapter studied the effect of catalyst contents and lactide monomer introduced to graft copolymerization reaction of PLA onto the modified EVA chains by catalytic reactive extrusion process with the help of tin (II) octoate ($Sn(Oct)_2$) catalyst, in order to initiate the graft copolymerization. Furthermore, the effect of screw configuration on the properties of EVA-g-PLA were studied.

6.3 Experimental

Materials

Ethylene (vinyl acetate) was supplied by TPI POLENE Public Co., Ltd. Polylactide (PLA), NatureWork, was purchased from Fresh bag Co., Ltd. Tin(II)-2-ethylhexanoate and Irganox® 1076 were purchased from SM Chemicals (Sigma Aldrich). Lactide monomer was purchased from Bio Invigor Inc., China.

Preparation of EVA-g-PLA with a combination of Lactide monomer

The preparation of EVA-g-PLA was done by catalytic reactive extrusion process in the twin-screw extruder from LabTech with L/D ratio of 20:1 (40-cm length and 2-cm diameter) and 2 die exits (3-mm diameter). The experiment will be done as follow: A mixture of modified EVA, PLA, and LA (the EVA to PLA to LA ratio 40:20:40) was mixed with $Sn(Oct)_2$ catalyst (0.1, 0.3 and 0.5%wt) and 0.5%wt of Irganox®1076 (antioxidant) before fed into the hopper. The barrel temperatures and screw rotating speeds were set as shown in Table 7.1. Throughput was melt

mixed again with the same extruder and the same condition in order to increase retention time. Then the throughput was dry in vacuum oven overnight at 60°C before characterizations. In order to investigate the suitable amount of catalyst and screw rotating speed, thermal properties, thermal stability, mechanical properties, and morphology of the throughput were examined. Moreover, the EVA-g-PLA without LA monomer produced from the previous chapter were also being in consider, in order to investigate any change after modification.

Preparation of EVA-g-PLA in a 5-mixing-zone twin-screw extruder (SHJ-36)

EVA-g-PLA of both two-component system (EVA and PLA, 40:60) and three-component system (EVA, PLA, and LA; 40:20:40), with a presence of $Sn(Oct)_2$ catalyst at various contents (0.1, 0.3, and 0.5 %wt) and 0.5%wt of antioxidant Irganox®1076, were produced by twin-screw extruder with 5 mixing zones, and screw diameter of 35.6 mm (Nanjing Giant Machinery Co., Ltd.) at screw rotating speed of 150 rpm for better mixing efficiency. The mixing conditions are shown in Table 6.1.

Characterizations

TG-DTA curves were collected on a Perkin-Elmer Pyris Diamond TG/DTA instrument. The sample was loaded on the platinum pan and heated from 30°C to 800°C at a heating rate of 10°C/min under N_2 flow.

DSC analysis were carried out using a METTLER TOLEDO DSC822 instrument. The sample was first heated from 30°C to 190°C and cooled down to -30°C at a rate of 10°C/min under a N_2 atmosphere with a flow rate of 25 ml/min. The sample was then reheated to 190°C at the same rate.

Scanning electron microscopy (SEM) was performed on Hitachi S-4800 Model. The samples were compressed into 3-mm-thickness sheets by compression moulding machine at 190°C, 10-minute preheating and 10-minute compression. Then the samples were cryogenic fractured in liquid nitrogen, in order to prevent mobility of polymer chains, and were coated by platinum (Pt) to make them electrically conductive.

Young's modulus, tensile strength, and % strain at break were measured according to ASTM D 882-91 using a Lloyd Mechanical Universal Testing Machine with a 500 N load cell, a 100.00 mm/min crosshead speed and a gauge length 50 mm.

Table 6.1 Mixing conditions of EVA-g-PLA

Type	Set Temperature (°C)										Screw speed (rpm)
	Z1	Z2	Z3	Z4	Z5	Z6	Z7	Z8	Z9	Die	
EVA:PLA (0.1, 0.3, and 0.5%wt)	140	150	160	165	165	165	165	165	165	160	30
	140	150	160	165	165	165	165	165	165	160	40
EVA:PLA:LA (0.1, 0.3, and 0.5%wt)	155	190	200	210	210	210	210	210	210	200	30
	155	190	200	210	210	210	210	210	210	200	40
EVA:PLA (0.1, 0.3, and 0.5%wt)	155	190	200	209	209	209	209	209	209	225	150
EVA:PLA:LA (0.1, 0.3, and 0.5%wt)	155	190	200	209	209	209	209	209	209	225	

6.4 Results and Discussion

6.4.1 Thermal Properties and Crystallization behaviors

Decomposition temperatures, melting temperatures and crystallization temperatures of the modified EVA-g-PLA produced at 30, 40 and 150 rpm with various catalyst contents are shown in Table 6.2.

Figure 6.1 showed TGA thermogram of EVA-g-PLA produced at 30 rpm, weight losses of the samples occurred in three steps, which related to the beginning compositions. The EVA-g-PLA produced at 40 rpm also show three steps in weight losses as can be seen in Figure 6.2, but not equivalent to the beginning

compositions, which was the evidence of non-homogeneous sample. Thermal stabilities of the copolymers produced at 30 and 40 rpm were lower than those of the pure EVA and pure PLA, due to the relatively low molecular weight fraction of the grafted chains [7]. Figure 6.3 showed TGA thermograms of EVA-g-PLA produced at 150 rpm, at 0.1 and 0.3%wt with no LA; and at 0.1%wt with LA, weight losses of the samples occurred in two steps, the first one around 310-320°C corresponded to degradation temperatures of PLA and vinyl acetate group of EVA, and the second one around 425-445°C corresponded to degradation temperature of ethylene chain.

DSC thermograms of EVA-g-PLA are shown in Figures (6.4-6.9). All samples showed two distinct melting peaks, one attributable to the melting of PLA crystallites (from 110 to 150°C), the second to ethylene crystallites (at about 70°C) [8]. These two melting peaks indicated the immiscibility of the samples [3]. Due to the conversion of graft copolymer was lower than those of the homopolymers [9]. T_m of the graft copolymer was lower than that of the neat PLA, as a result of complex structure and relatively low molecular weight of PLA side chains [5].

Table 6.2 Thermal Properties of EVA-g-PLA produced at 30 and 40 rpm with various catalyst contents (0.1, 0.3, and 0.5 %wt)

$Sn(Oct)_2$ (%wt)	Decomposition Temperature			Melting Temperature				Crystallinity (%)		Crystallization Temperature	
	1st	2nd	3rd	1st peak	ΔH (J/g)	2nd peak	ΔH (J/g)	1st peak	2nd peak	Onset (°C)	Peak (°C)
Pure EVA	-	310.7	429.5	68.84	16.59	-	-	5.66	-	61.73	53.87
Pure PLA	-	332.5	-	-	-	151.28	38.01	-	40.87	-	-
EVA-g-PLA at 30 rpm											
0.1	258.1	328.6	428.7	71.86	53.23	143.22	41.38	18.17	44.49	62.95	54.16
0.3	249.8	321.1	428.5	95.27	53.40	144.67	39.43	18.23	42.40	62.62	54.82
0.5	244.6	317.5	430.3	70.49	26.15	144.94	39.4	8.92	42.36	104.82, 62.19	94.23, 54.36
EVA-g-PLA at 40 rpm											
0.1	258.3	320.7	431.8	73.32	7.47	119.11	9.11	2.55	9.80	59.72	54.20
0.3	241.7	316.9	429.2	72.52	6.19	126.15	5.84	2.11	6.28	60.20	54.32
0.5	248.7	321.6	430.7	72.37	13.46	122.99	15.08	4.59	16.22	61.06	54.78

Table 6.3 Thermal Properties of EVA-g-PLA produced at 150 rpm with various catalyst contents (0.1, 0.3, and 0.5 %wt)

Screw speed	$Sn(Oct)_2$ (%wt)	Decomposition Temperature(°C)			Melting Temperature (°C)				Crystallinity (%)		Crystallization Temperature	
		1st	2nd	3rd	1st peak	ΔH (J/g)	2nd peak	ΔH (J/g)	1st peak	2nd peak	Onset (°C)	Peak (°C)
Pure EVA		-	310.7	429.5	68.84	16.59	-	-	5.66	-	61.73	53.87
Pure PLA		-	332.5	-	-	-	151.28	38.01	-	40.87	-	-
EVA:PLA:LA	0.1	244.9	321.7	430.6	61.19	41.75	113.95	35.85	14.25	38.55	61.41	54.85
at 30 rpm	0.3	260.8	324.8	431.2	66.56	47.55	115.49	44.69	16.23	48.05	61.16	54.64
	0.5	239.7	319.5	430.7	69.54	35.20	120.68	23.27	12.01	25.02	60.53	54.34
EVA:PLA:LA	0.1	254.6	321.2	430.5	70.23	5.37	117.71	4.35	1.83	4.68	60.39	54.77
at 40 rpm	0.3	253.0	323.5	431.9	72.23	5.7	118.69	14.17	1.94	15.24	60.58	54.61
	0.5	258.5	320.7	430.5	70.06	42.74	120.04	6.29	14.59	6.76	62.15	56.24
EVA:PLA	0.1	-	317.3	445.3	65.84	3.25	150.06	4.06	1.11	4.36	116.44	66.65
at 150 rpm	0.3	-	326.3	428.9	65.50	4.09	149.57	2.16	1.40	2.32	73.73	66.63
	0.5	254.5	316.1	428.6	64.47	16.49	150.77	3.90	5.63	4.19	115.64	66.62
EVA:PLA:LA	0.1	-	309.0	430.4	79.5	14.50	132.75	1.65	4.95	1.77	61.11	55.30
at 150 rpm	0.3	256.1	318.2	430.7	67.02	7.82	134.57	23.98	2.67	25.78	60.78	54.82
	0.5	262.4	318.0	431.9	59.70	7.10	147.73	15.36	2.42	16.52	93.79	59.12

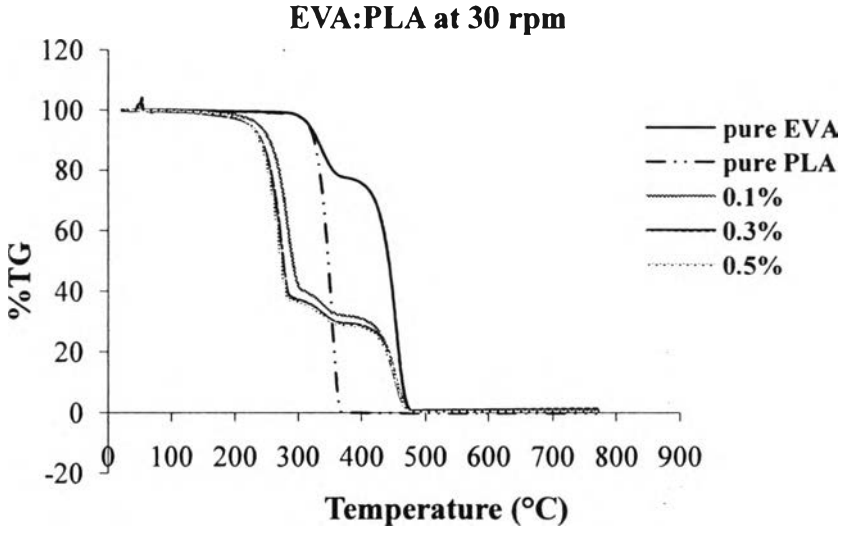

(a)

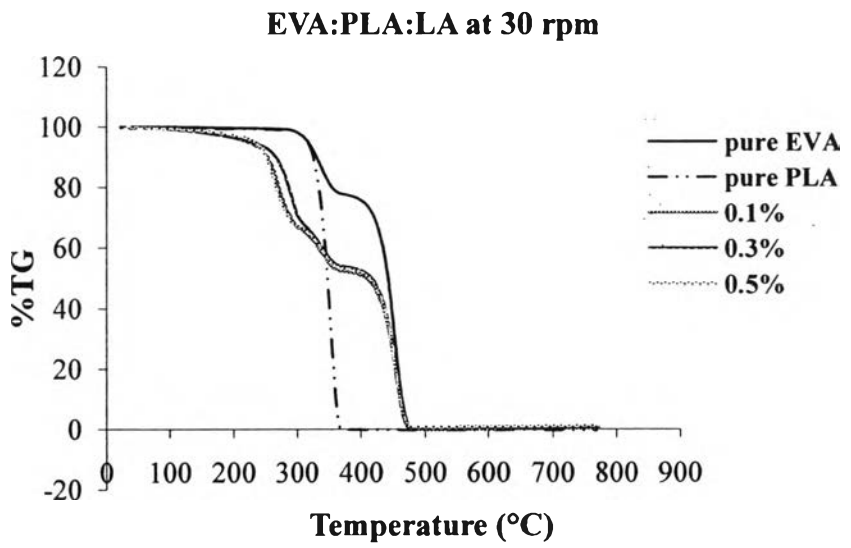

(b)

Figure 6.1 TGA plots of EVA-g-PLA at 30 rpm with various catalyst contents (0.1, 0.3, and 0.5%wt); (a) EVA:PLA, 40:60, (b) EVA:PLA:LA, 40:20:40.

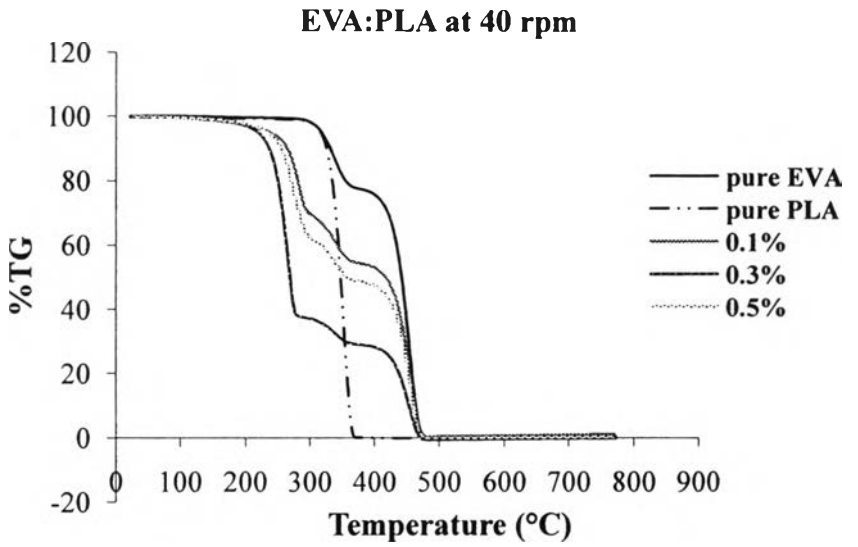

(a)

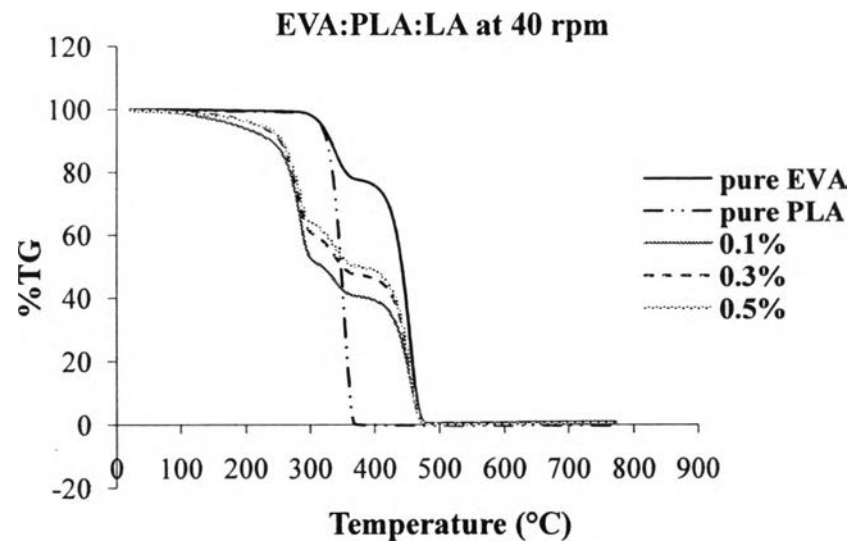

(b)

Figure 6.2 TGA plots of EVA-g-PLA at 40 rpm with various catalyst contents (0.1, 0.3, and 0.5%wt); (a) EVA:PLA:LA, 40:60, (b) EVA:PLA:LA, 40:20:40.

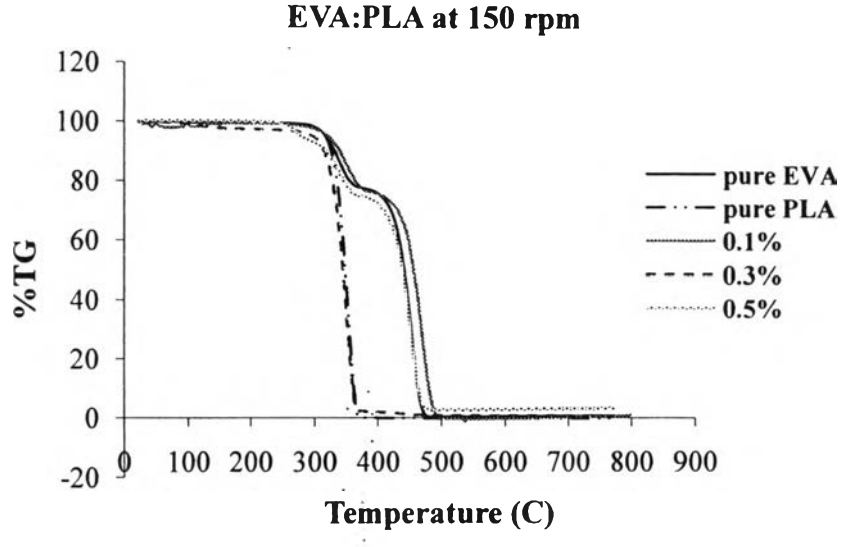

(a)

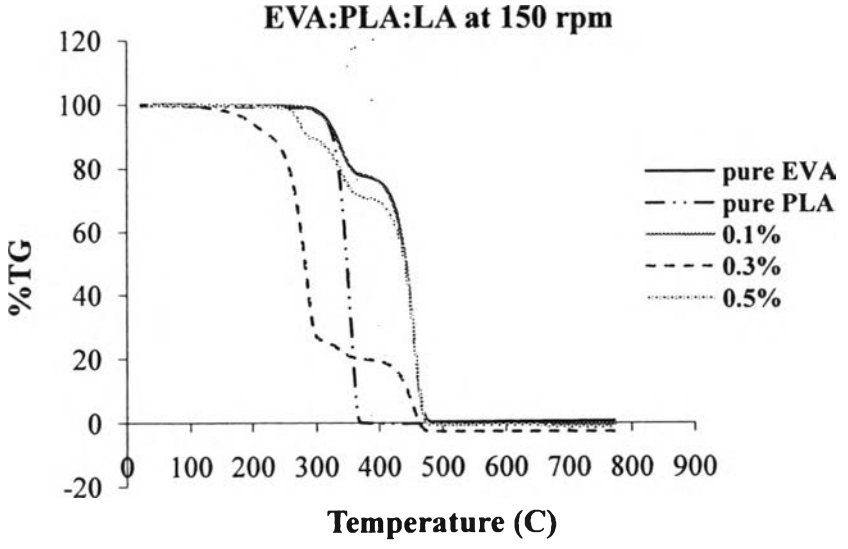

(b)

Figure 6.3 TGA plots of EVA-g-PLA at 150 rpm with various catalyst contents (0.1, 0.3, and 0.5%wt); (a) EVA:PLA, 40:60, (b) EVA:PLA:LA, 40:20:40.

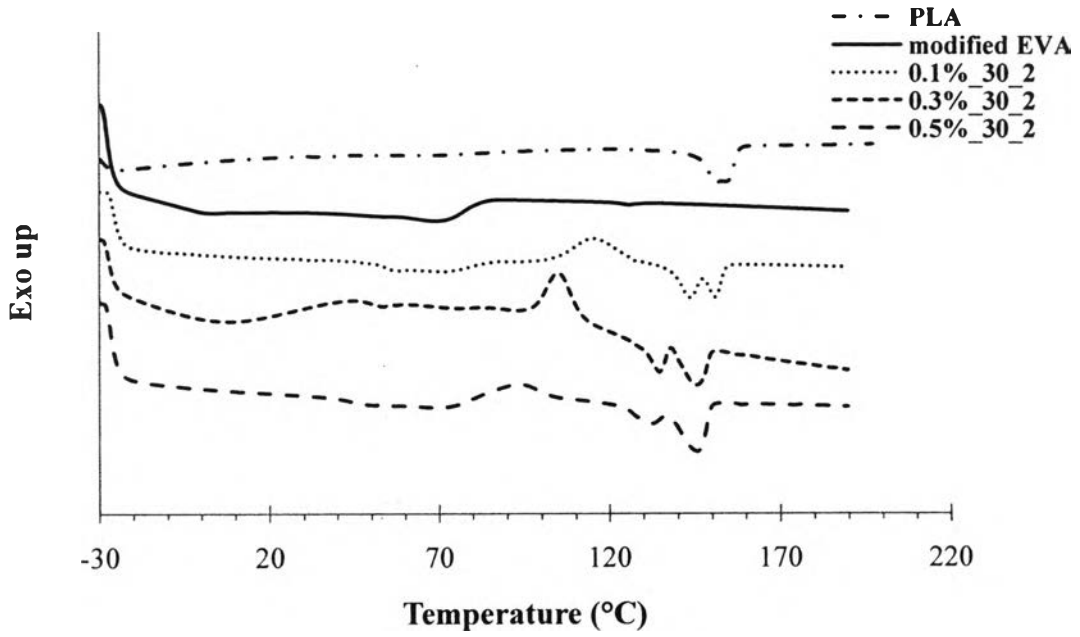

(a)

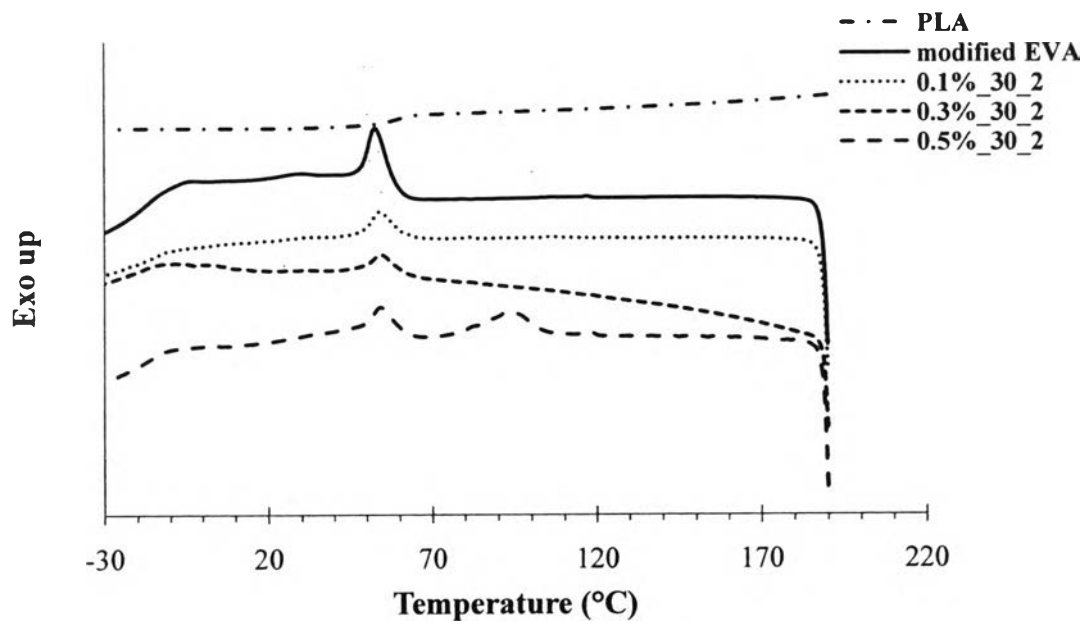

(b)

Figure 6.4 DSC thermograms of EVA-g-PLA (EVA:PLA, 60:40) at 30 rpm with various catalyst contents (0.1, 0.3, and 0.5%wt); (a) endotherm (2^{nd} heating), (b) exotherm.

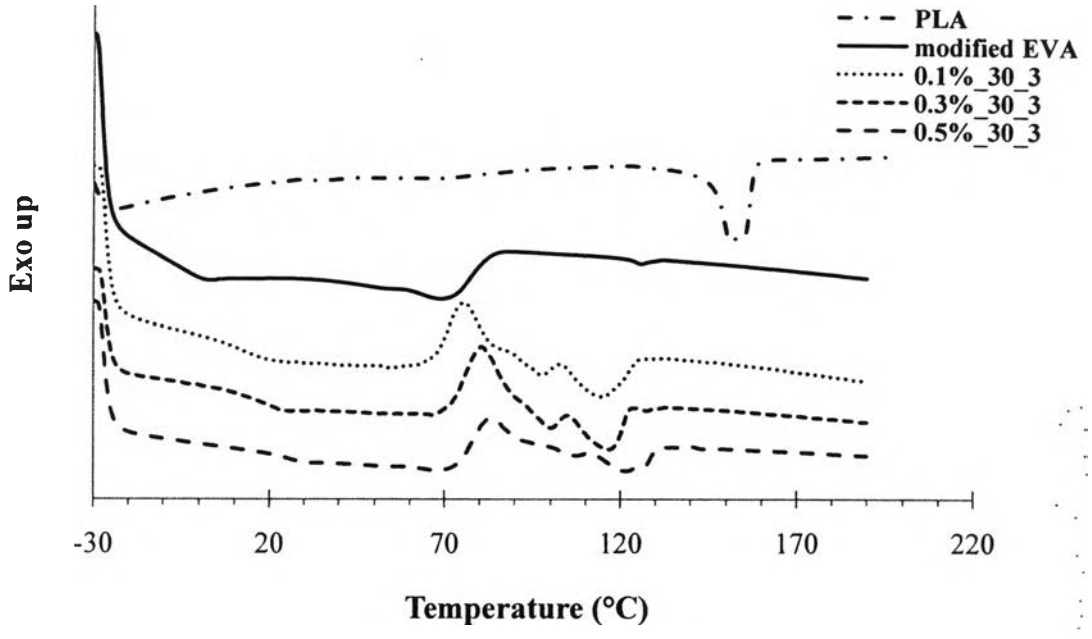

(a)

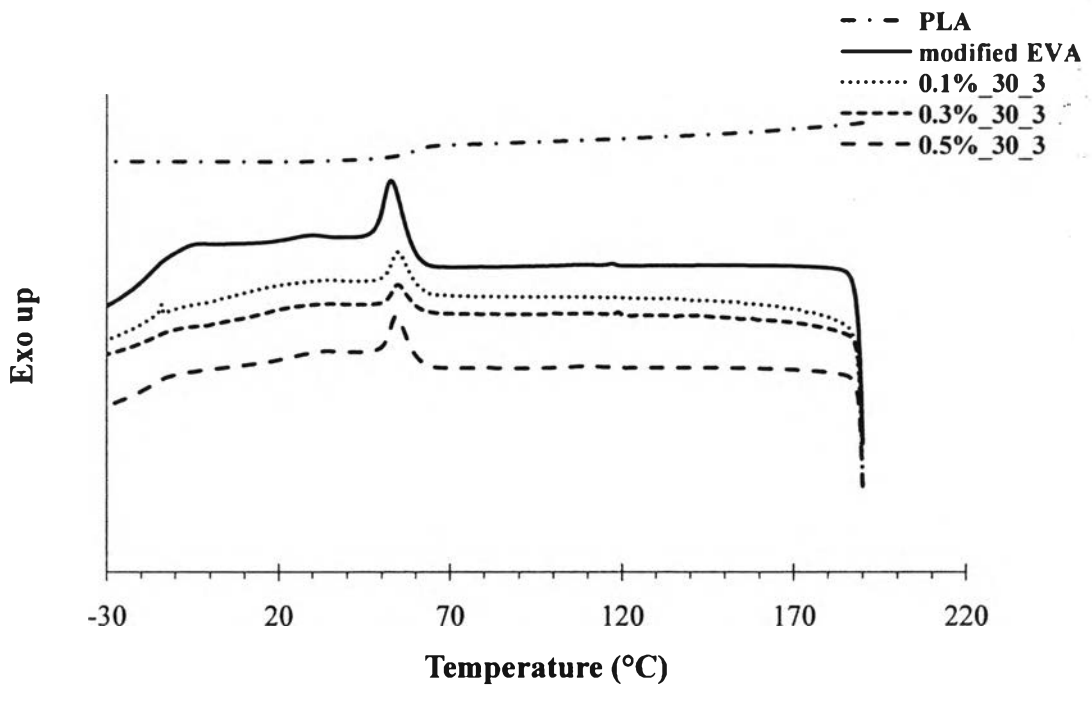

(b)

Figure 6.5 DSC thermograms of EVA-g-PLA (EVA:PLA:LA, 60:20:40) at 30 rpm with various catalyst contents (0.1, 0.3, and 0.5%wt); (a) endotherm (2nd heating), (b) exotherm.

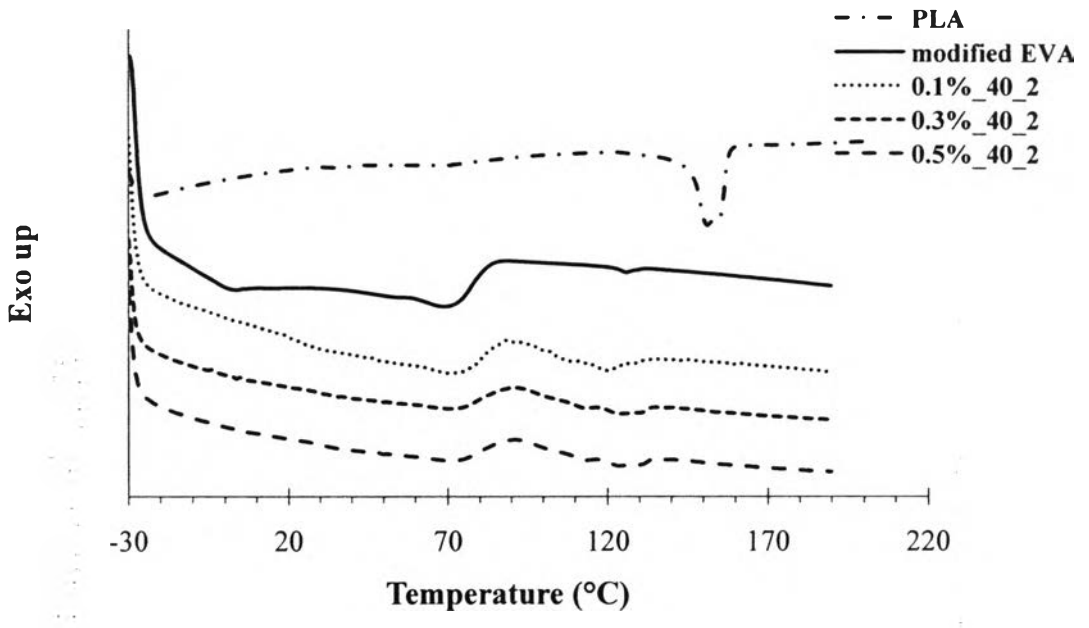

(a)

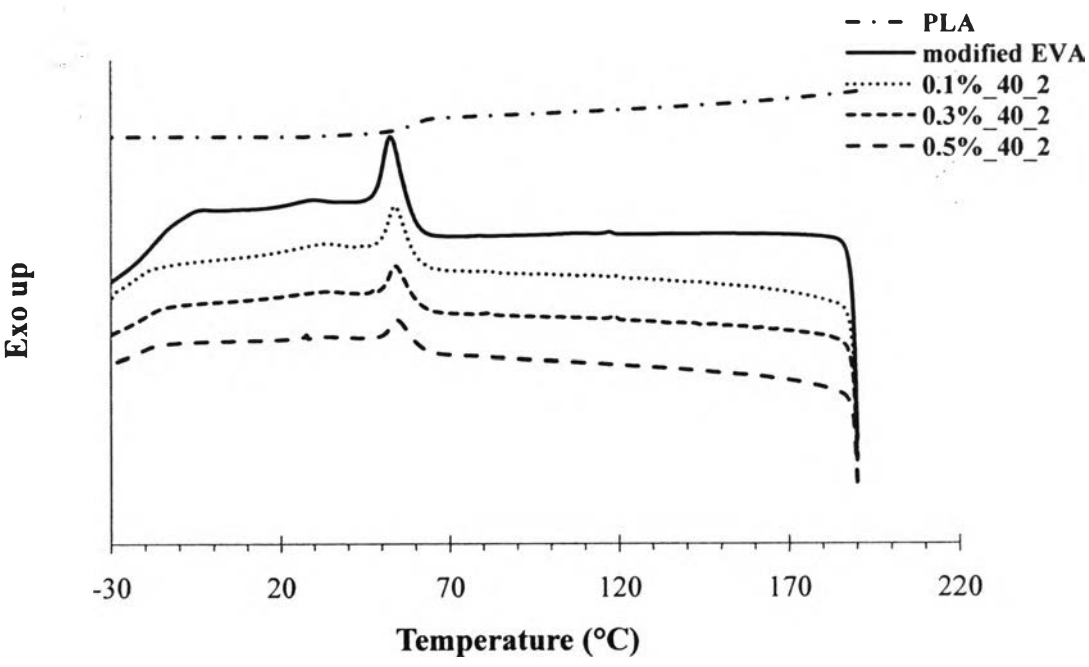

(b)

Figure 6.6 DSC thermograms of EVA-g-PLA (EVA:PLA, 60:40) at 40 rpm with various catalyst contents (0.1, 0.3, and 0.5%wt); (a) endotherm (2^{nd} heating), (b) exotherm.

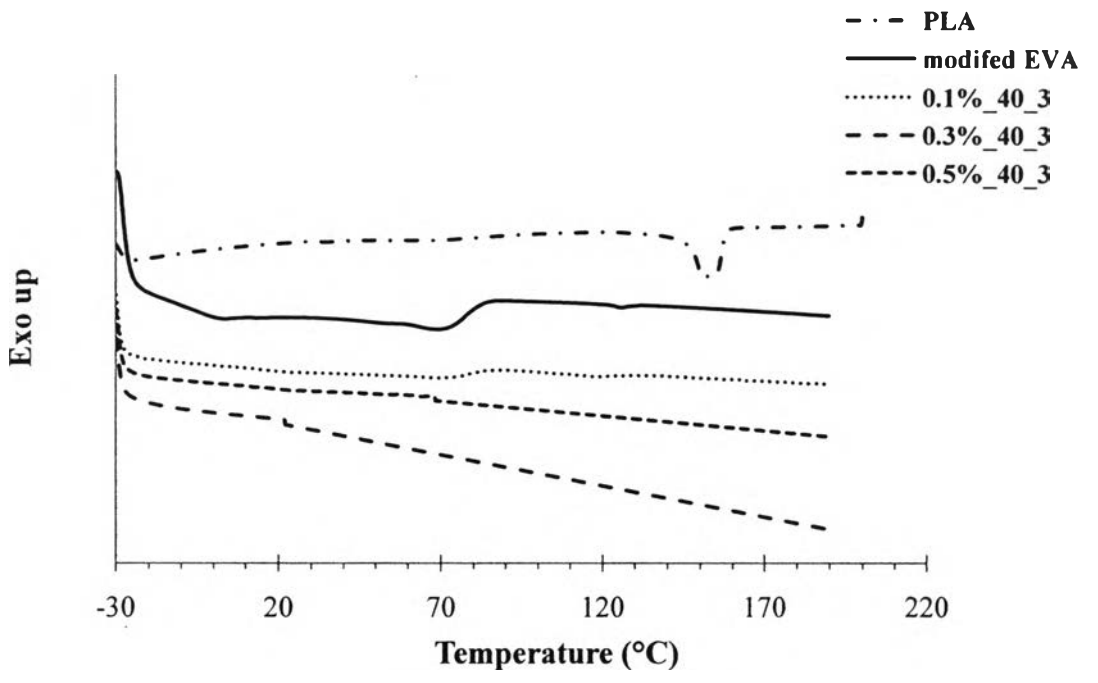

(a)

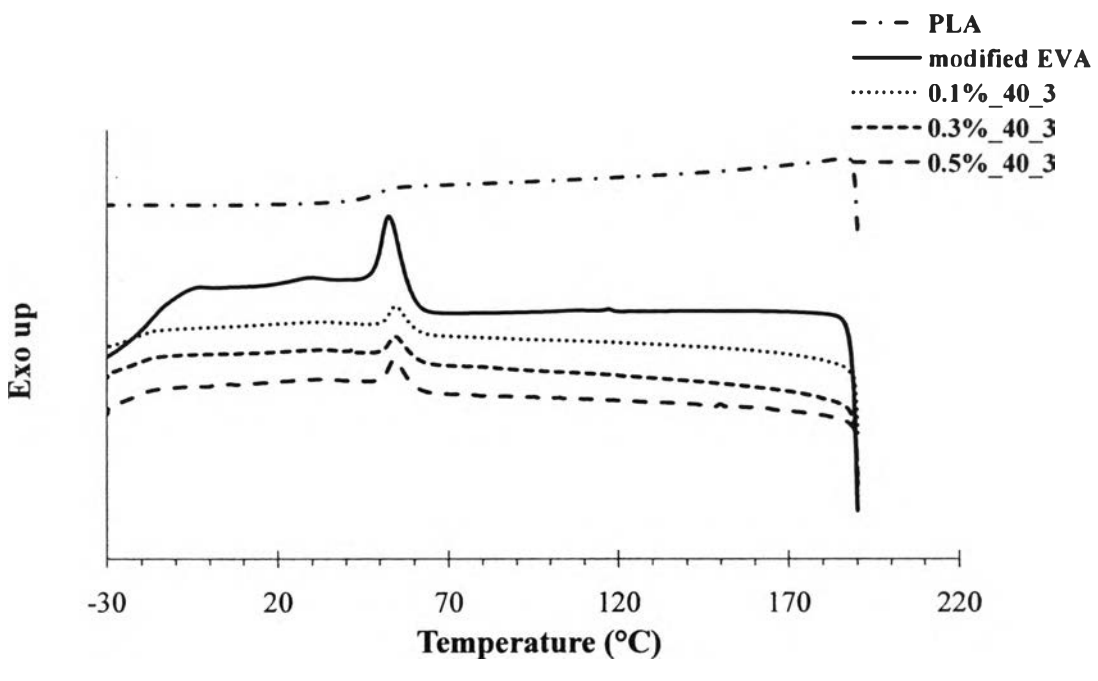

(b)

Figure 6.7 DSC thermograms of EVA-g-PLA (EVA:PLA:LA, 60:20:40) at 40 rpm with various catalyst contents (0.1, 0.3, and 0.5%wt); (a) endotherm (2nd heating), (b) exotherm.

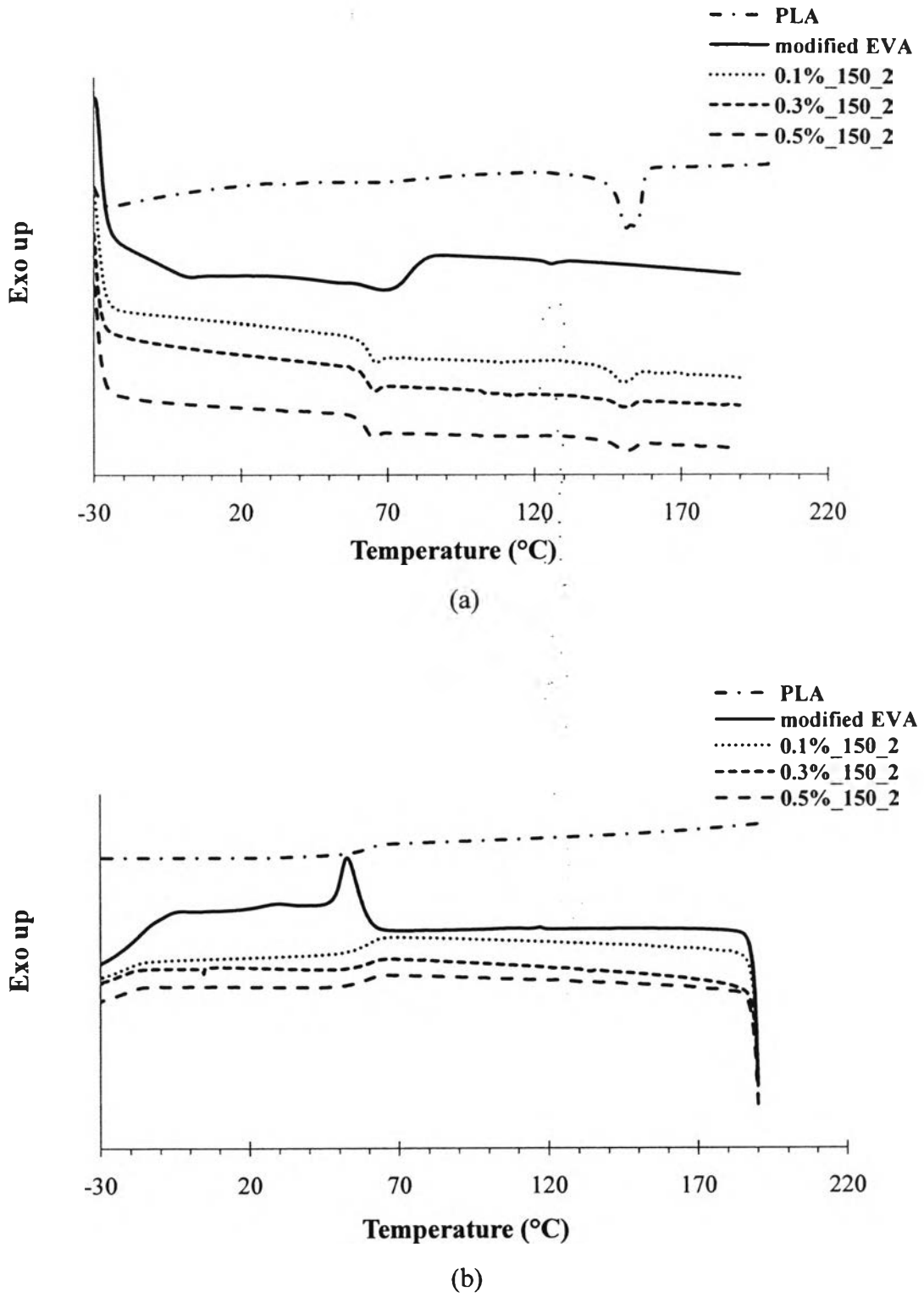

Figure 6.8 DSC thermograms of EVA-g-PLA (EVA:PLA, 60:40) at 150 rpm with various catalyst contents (0.1, 0.3, and 0.5%wt); (a) endotherm (2^{nd} heating), (b) exotherm.

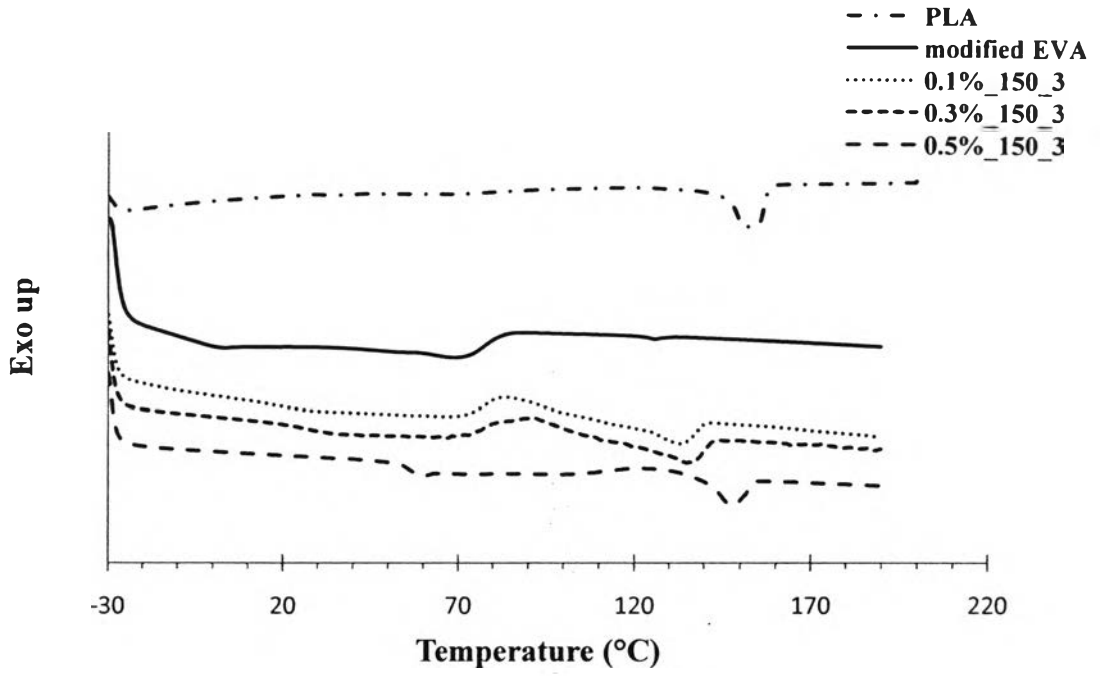

(a)

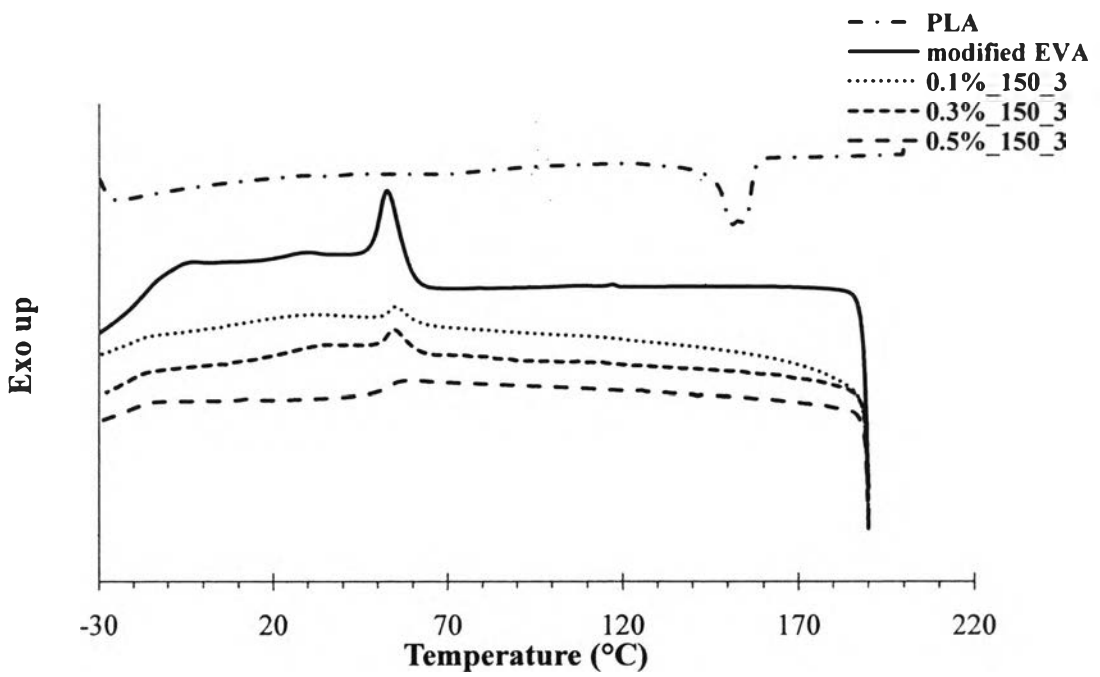

(b)

Figure 6.9 DSC thermograms of EVA-g-PLA (EVA:PLA:LA, 60:20:40) at 150 rpm with various catalyst contents (0.1, 0.3, and 0.5%wt); (a) endotherm (2^{nd} heating), (b) exotherm.

6.4.2 Morphology

SEM

According to the morphology of EVA-g-PLA from SEM micrograph (Chapter VI), where phase separation can be seen, the lactide monomer was introduced into the mixture, in order to initiate the graft copolymerization by ring-opening process of lactide. The morphology of EVA-g-PLA (EVA:PLA:LA) with the help of various catalyst contents (0.1, 0.3, and 0.5%wt) were investigated.

Although lactide monomer (LA) was added, phase separation was still observed in all samples, as shown in Figures (6.10 and 6.11). Therefore, the reaction was took place in the different modular twin screw extruder with five mixing zones, in order to improve mixing efficiency leading to higher conversion of graft copolymer. However, phase separation was still observed even in a present of LA as shown in Figure 6.12. The reason for phase separation was possibly due to the homopolymerization reaction was taking place in competition with the copolymerization reaction, which resulted in formation of more homopolymer [10] and lower graft copolymer leading to lower compatibility between EVA and PLA phases.

The EVA-g-PLA produced at 30 and 40 rpm were fabricated by the same twin-screw extruder from LabTech, their morphology are shown in Figures (6.10 and 6.11). The phase separations are highly pronounced in EVA-g-PLA produced at 40 rpm (Figure 6.11), this might be a result of lower conversion of graft copolymer due to the higher screw speed [11]. Figures 6.10 (a) and Figure 6.10 (d) show that the catalyst content of 0.1%wt might not suitable for producing a desire amount of EVA-g-PLA, this caused phase separation to occur. Figure 6.10 (c) and Figure 6.10 (f) show that the catalyst content of 0.5%wt might be exceeded, which was subjected to homopolymerization of PLA [12]. Where the finest dispersion was found in EVA-g-PLA produced at 30 rpm with 0.3%wt catalyst, due to the effect of an interfacial interaction that caused by the formation of the graft copolymer [13].

SEM images in Figure 6.12 show morphology of the EVA-g-PLA produced at 150 rpm was fabricated by SHJ-36 twin-screw extruder with 5 mixing zones, and screw diameter of 36 mm from Nanjing Giant Machinery Co., Ltd. Figure

6.12 (a) and Figure 6.12 (c) indicated that the conversion of graft copolymer was high enough for the interfacial interaction between homo-PLA and homo-EVA to take place [13] which resulted in the smooth interface that fused into the matrix.

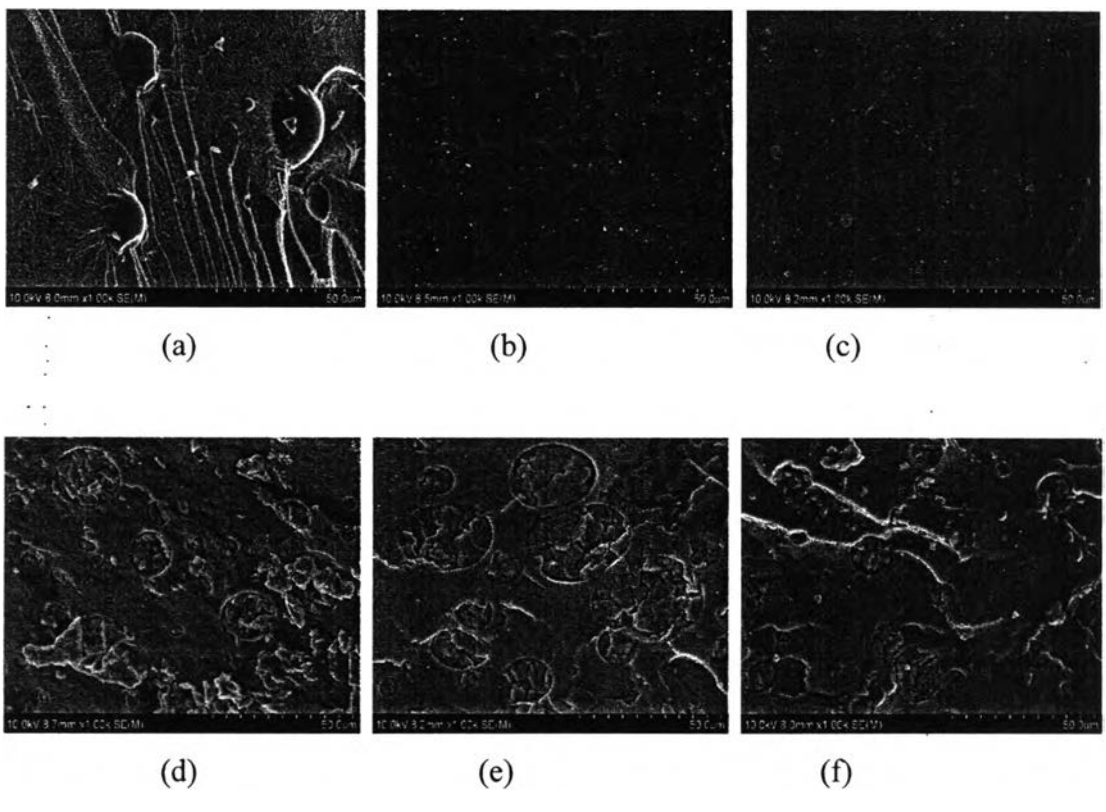

Figure 6.10 SEM images of EVA-g-PLA at screw speed of 30 rpm and various catalyst contents; (EVA:PLA) (a) 0.1%wt, (b) 0.3%wt, and (c) 0.5%wt; (EVA:PLA:LA) (d) 0.1%wt, (e) 0.3%wt, and (f) 0.5%wt.

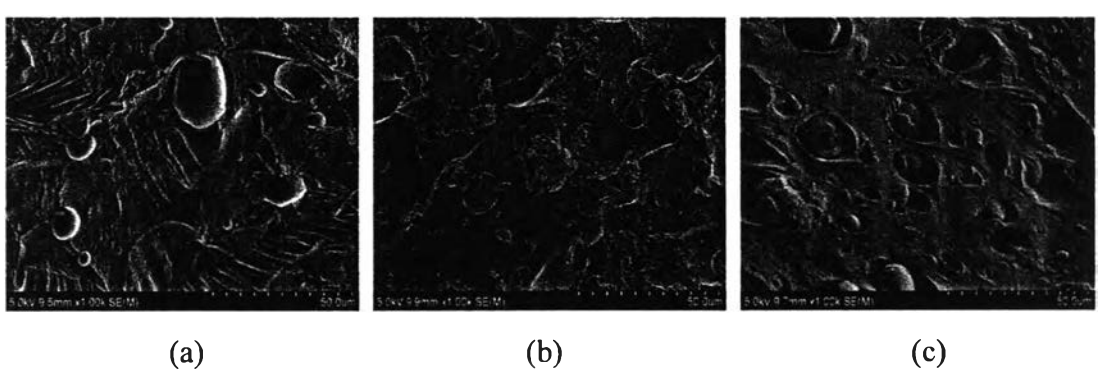

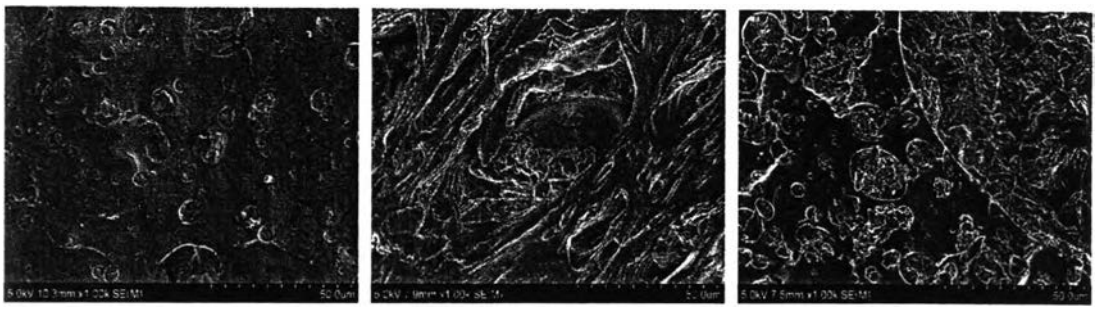

(d) (e) (f)

Figure 6.11 SEM images of EVA-g-PLA at screw speed of 40 rpm and various catalyst contents; (EVA:PLA) (a) 0.1%wt, (b) 0.3%wt, and (c) 0.5%wt; (EVA:PLA:LA) (a) 0.1%wt, (b) 0.3%wt, and (c) 0.5%wt.

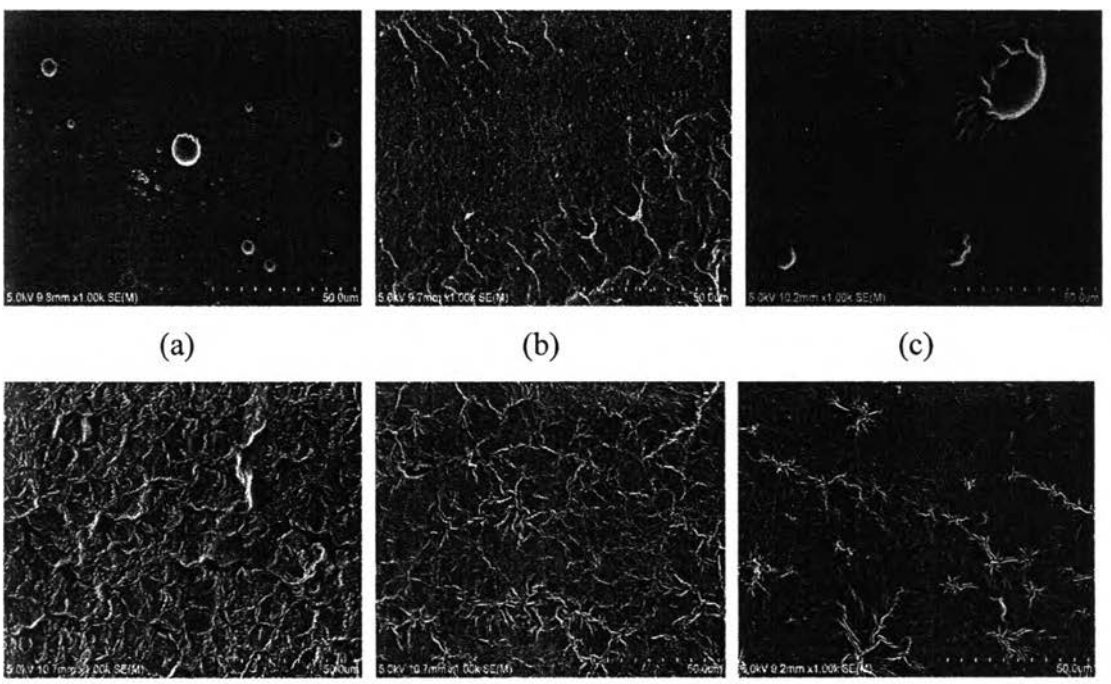

(a) (b) (c)

(d) (e) (f)

Figure 6.12 SEM images of EVA-g-PLA at 150 rpm and various catalyst contents; (EVA:PLA) (a) 0.1%wt, (b) 0.3%wt, and (c) 0.5%wt; (EVA:PLA) (a) 0.1%wt, (b) 0.3%wt, and (c) 0.5%wt.

6.4.3 Mechanical Properties

Tensile Properties Testing

Tensile Properties of EVA-g-PLA produced from various catalyst contents (0.1, 0.3 and 0.5%wt) at screw rotating speeds of 30, 40 and 150 rpm are shown in Table 6.4.

Figure 6.13, EVA-g-PLA (with no LA) produced at 30 rpm with 0.1%wt $Sn(Oct)_2$ give the highest Young's modulus, where it presents the lowest % strain at break, due to the crystalline parts of the sample acts like hard segments resulting in chain stiffness, which not allow it to stretch long [14], while tensile strength of the samples are not much different. For EVA-g-PLA produced at 40 rpm, the sample with 0.1%wt $Sn(Oct)_2$ was too brittle to be examined. The sample with 0.3%wt $Sn(Oct)_2$ give higher Young's moduls than the sample with 0.5%wt, but it presents lower tensile strenght and % strain at break. The EVA-g-PLA (with LA) produced at 30 and 40 rpm exhibit lower Young's modulus than those produced without LA, the reason might because of lower molecular weight of PLA segment and lower % crystallinity, where tensile strength of the samples are slightly higher than those without LA. The EVA-g-PLA produced at 30 rpm with a present of LA give the highest % strain at break, due to the plasticization effect of oligomeric PLA. But the EVA-g-PLA produced at 40 rpm (with LA) show the lowest % strain at break, as a result of phase separation, since the formation of graft copolymer was lower than homopolymer. The EVA-g-PLAproduced at 150 rpm (without LA) with 0.3%wt $Sn(Oct)_2$ give the best results in tensile test when compare with the same series, as shown in Figure 6.14. The EVA-g-PLA produced at 150 rpm with a present of LA at 0.5%wt $Sn(Oct)_2$ cannot be determined because of its brittleness, where the other two samples (0.1, and 0.3%wt) present lower Young's modulus and tensile strength but higher in % strain at break. The reason is possibly due to sample preparation, which result in non-homogeneous specimens.

Table 6.4 The tensile testing results of EVA-g-PLA at various catalyst contetnts

Screw Speed (rpm)	Catalyst Content (wt%)	Young's Modulus (MPa)	Tensile Strength (MPa)	%Strain at Break
	EVA+PLA			
30	0.1	38.31(±16.2)	0.68(±0.09)	299.76(±58.7)
	0.3	28.98(±4.3)	1.12(±0.06)	498.74(±23.0)
	0.5	27.87(±8.9)	0.92(±0.10)	377.94(±46.01)
	EVA+PLA			
40	0.1	-	-	-
	0.3	36.17(±5.5)	0.10(±0.09)	448.88(±47.2)
	0.5	17.27(±1.6)	1.88(±0.09)	605.62(±34.6)
	EVA+PLA+LA			
	0.1	18.94(±1.3)	1.97(±0.13)	758.5(±35.6)
30	0.3	20.43(±2.6)	1.55(±0.13)	836.36(±53.7)
	0.5	25.82(±2.8)	1.38(±0.36)	730.26(±26.8)
	EVA+PLA+LA			
	0.1	12.51(±2.2)	1.61(±0.11)	699.77(±36.4)
40	0.3	20.03(±2.1)	1.10(±0.02)	628.66(±46.8)
	0.5	19.10(±3.9)	1.36(±0.10)	689.67(±28.9)
	EVA+PLA			
	0.1	1675.32(±101.26)	2.43(±0.25)	1.143(±0.09)
150	0.3	2191.49(±130.31)	8.05(±0.59)	5.67(±4.08)
	0.5	1948.9(±96.78)	3.81(±0.34)	1.28(±0.32)
	EVA+PLA+LA			
150	0.1	26.32(±3.92)	1.37(±0.11)	699.56(±53.48)
	0.3	60.80(±27.46)	1.14(±0.07)	467.12(±36.59)
	0.5	-	-	-
PLA		1817.66(±117.29)	10.88(±1.01)	5.20(±0.21)
Modified EVA		11.69(±0.54)	1.75(±0.08)	871.5(±26.61)

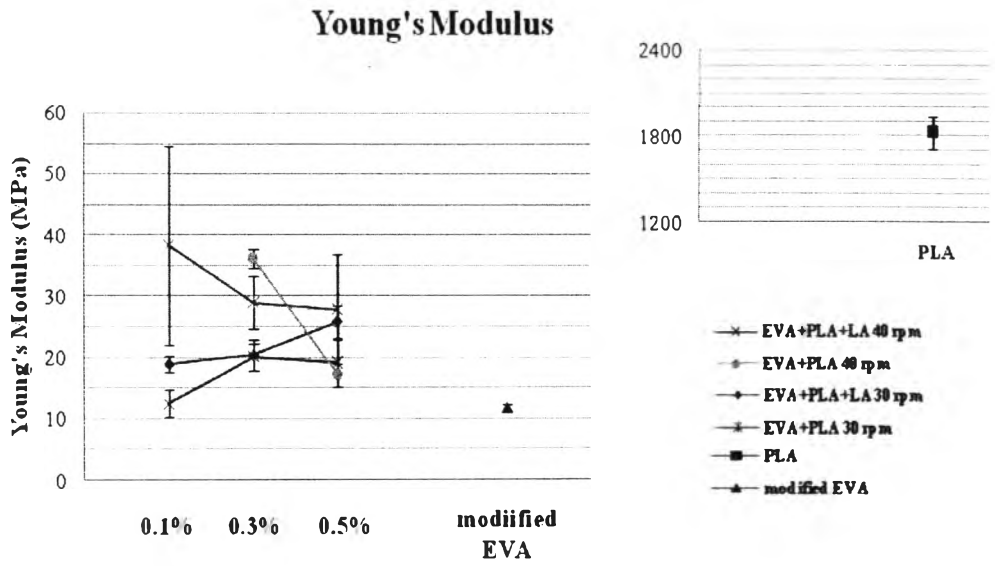
Young's Modulus
Young's Modulus (MPa)
60
50
40
30
20
10
0
0.1%
0.3%
0.5%
modiified EVA
2400
1800
1200
PLA
EVA+PLA+LA 40 rpm
EVA+PLA 40 rpm
EVA+PLA+LA 30 rpm
EVA+PLA 30 rpm
PLA
modified EVA

(a)

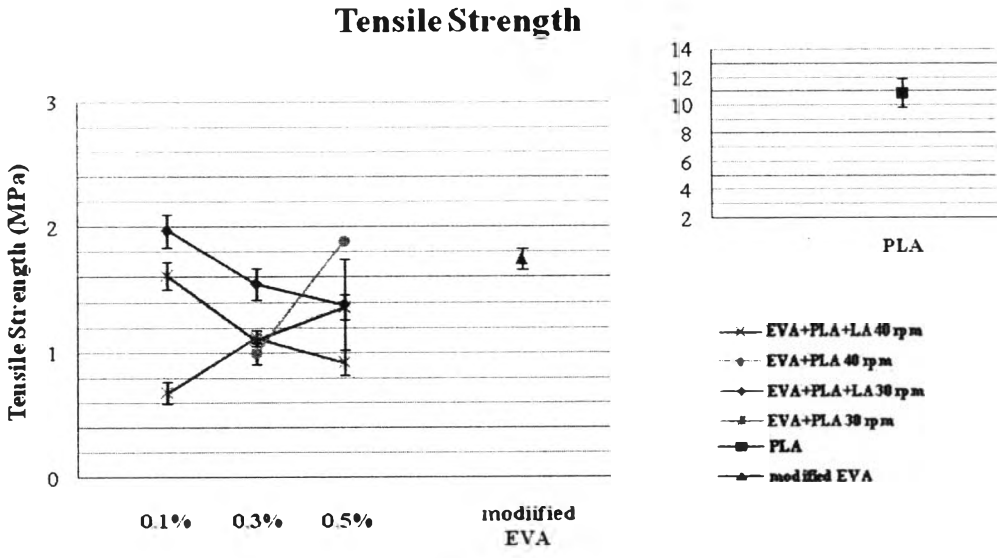
Tensile Strength
Tensile Strength (MPa)
3
2
1
0
0.1%
0.3%
0.5%
modiified EVA
14
12
10
8
6
4
2
PLA
EVA+PLA+LA 40 rpm
EVA+PLA 40 rpm
EVA+PLA+LA 30 rpm
EVA+PLA 30 rpm
PLA
modified EVA

(b)

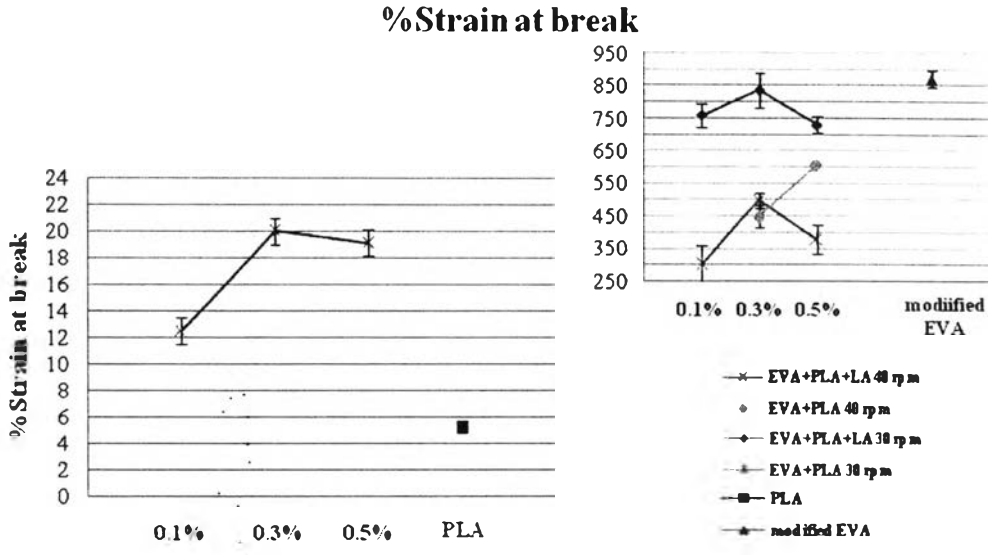

(c)

Figure 6.13 Tensile test of EVA-g-PLA, with 0%wt LA and 40%wt LA, produced at 30 and 40 rpm and at various catalyst contents (0.1, 0.3, and 0.5%wt); (a) Young's modulus, (b) Tensile strength, (c) % Strain at break.

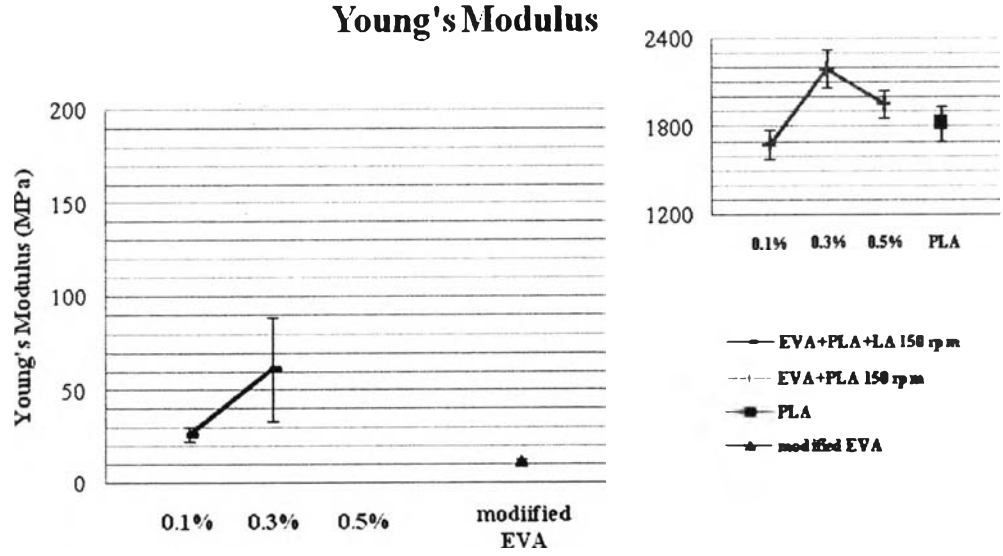

(a)

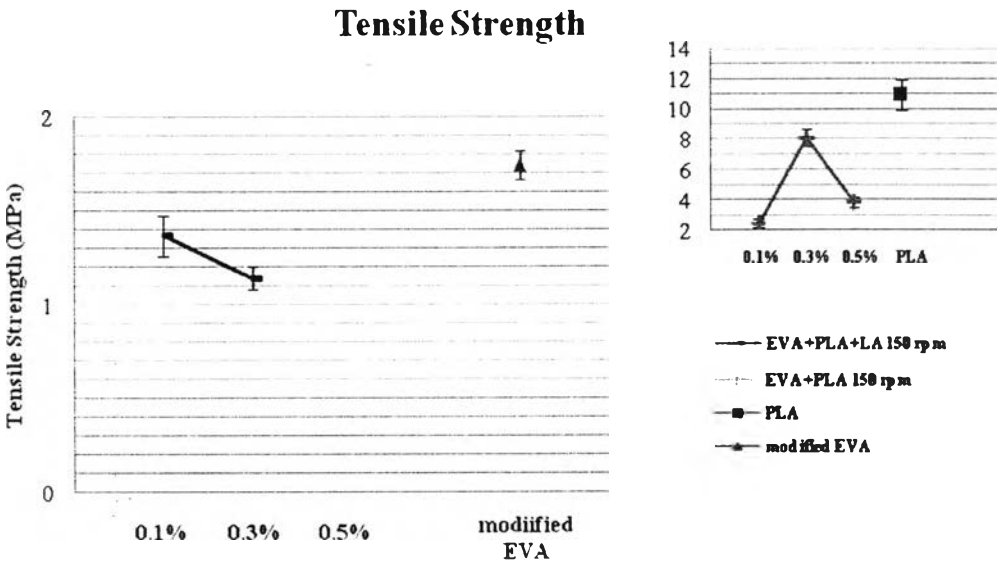

(b)

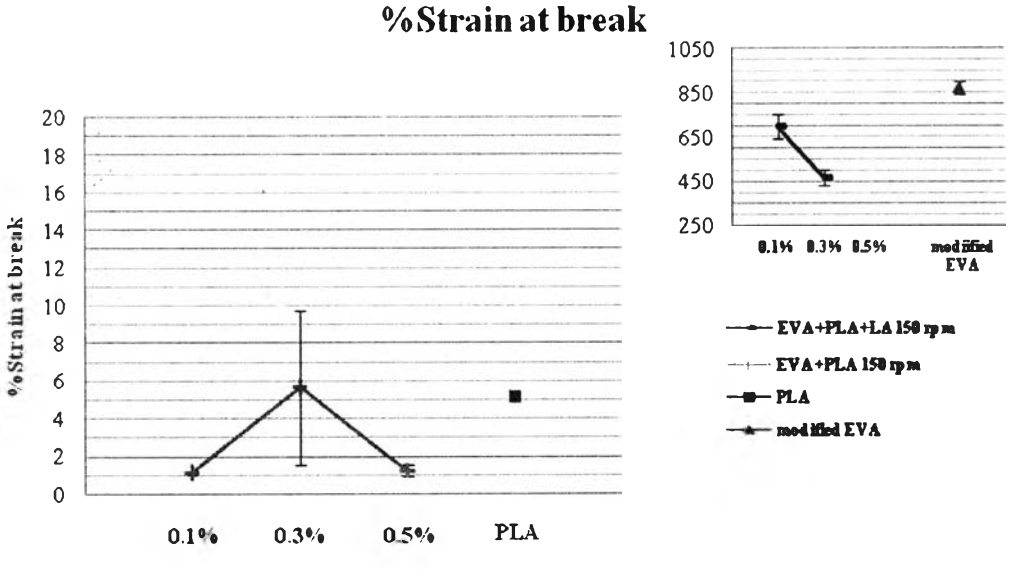

(c)

Figure 6.14 Tensile test of EVA-g-PLA, with 0%wt LA and 40%wt LA, produced at 150 rpm and various catalyst contents (0.1, 0.3, and 0.5%wt); (a) Young's modulus, (b) Tensile strength, (c) % Strain at break.

6.5 Conclusions

The introduction of lactide monomer could not make any significant improvement on the morphology of the graft copolymer at screw rotating speed of 40 rpm. But the considerable morphology was highly pronounced when it was mixed in a five-mixing zone extruder at screw speed of 150 rpm with 0.3%wt of $Sn(Oct)_2$ and no LA, which showed the finest dispersion as well as the graft copolymer produced with 0.3%wt $Sn(Oct)_2$ at 30 rpm without LA. As a result, the highest conversion of EVA-g-PLA, which worked as a compatibilizer, increased interfacial activity of both EVA and PLA homopolymers. Therefore, the suitable amount of catalyst and screw speed are 0.3%wt $Sn(Oct)_2$ and 30 rpm and/or 150 rpm, respectively.

6.6 Acknowledgements

I would like to thank TPI POLENE Public Company limited for material support, and Jobthai Industry Company Limited for provide the instruments support.

Moreover, I gratefully acknowledge the help of Assoc. Prof. Rathanawan Magaraphan, Dr.Thanyalak Chaisuwan and Asst. Prof. Suparat Rukchonlatee for their suggestion of the experiment.

Finally, the author is grateful for the funding of the thesis work provided by the Petroleum and Petrochemical College; The National Center for Petroleum, Petrochemicals, and Advanced Materials; and Polymer Processing and Polymer nanomaterial research unit.

6.7 References

[1] Qi, F., and Hanna, M.A. (1999) Rheological Properties of Amorphous and Semicrystalline Polylactic Acid Polymers. Industrials Crops and Products, 10, 47-53.

[2] Ogata, N., Jimenez, G., Kawai, H., and Ogihara, T.J. (1997) Structure and thermal/mechanical properties of poly (l-lactide)-clay blend, Journal of Polymer Science part B: Polymer Physics, 35, 389-396.

[3] Bhatia, A., Y., Rahul, K.G., Bhattacharya, S.N., and Choi, H.J. (2007) Compatibility of Biodegradable Poly(lactic acid) (PLA) and Poly(butylene

succinate) (PBS) Blends for Packaging Application. Korea-Australia Rheology Journal, 19, 125-131.

[4] Becquart, F., Taha, M., Zerroukhi, A., Kaczun, J., and Llauro, M.F. (2007) Microstructure and properties of poly(vinyl alcohol-co-vinyl acetate)-g-ε-caprolactone. European Polymer Journal, 43, 1549-1556.

[5] Jiang, H., He, J., Liu, J., and Yang, Y. (2002) Synthesis and characterization of poly(ethylene-co-vinyl alcohol)-graft-poly(epsilon-caprolactone). Polymer Journal, 34, 682-686.

[6] Moraes, M. A. R., Moreira, A. C. F., Barbosa, R. V., and Soares, B. G. (1996) Graft Copolymer from Modified Ethylene−Vinyl Acetate (EVA) Copolymers. 3. Poly(EVA-g-Methyl Methacrylate) from Mercapto-Modified EVA. Macromolecules, 29, 416–422.

[7] Ikada, Y., and Tsuji, H. (2000) Biodegradable Polyesters for Medical and Ecological Applications. Macromolecular Rapid Communications, 21, 117-132.

[8] Brown, S.B. (1991). Annual Reviews of Material Science, 21, 409-35.

[9] Finkenstadt, V.L., and Willet, J.L. (2005) Reactive Extrusion of Starch-Polyacrylamide Graft Copolymers: Effects of Monomer/Starch Ratio and Moisture Content. Macromolecular Chemistry and Physics, 206, 1648-1652.

[10] Hanley, S.J., Nesheiwat, A.M., Chen, R.T, Jamieson, M., Pearson, R.A., Sperling, L.H. (2000) Phase Separation in Semicrystalline Blends of Poly(phenylene sulfide) and Poly(ethylene terephthalate). II. Effect of Poly(phenylene sulfide) Homopolymer Solubilization of PPS-graft-PET Copolymer on Morphology and Crystallization Behavior. Journal of Polymer Science, 38(4), 599-610.

[11] Zhu, W., Jaluria, Yo. (2004) Residence time and conversion in the extrusion of chemically reactive materials. Polymer Engineering and Science, 41, 1280-1291.

[12] Chen, L., Qiu, X., Deng, M., Hong, Z., Luo, R., Chen, X., and Jing, X. (2005) The starch grafted poly(L-lactide) and the physical properties of its blending composites. Polymer, 46, 5723-5729.

[13] Young, F.K., Chang, N.C., Young, D.K., Ki, Y.L., and Moo, S.L. (2004) Compatibilization of Immiscible Poly(*l*-lactide) and Low Density Polyethylene Blends. Fibers and Polymers, 5, 270-274.